Available online at www.sciencedirect.com
ScienceDirect
Journal of Magnetic Resonance 191 (2008) 282–290
JMR Journal of Magnetic Resonance
www.elsevier.com/locate/jmr

Improved diffusion-weighting efficiency of pulsed gradient stimulated echo MR measurements with background gradient cross-term suppression

Jürgen Finsterbusch *

Department of Systems Neuroscience, University Medical Center Hamburg–Eppendorf, Hamburg, Germany
Neuroimage Nord, University Medical Centers Hamburg–Kiel–Lübeck, Germany

Received 26 October 2007; revised 7 January 2008
Available online 10 January 2008

Abstract

Accurate diffusion measurements with pulsed gradient NMR are hampered by cross-terms of the diffusion-weighting and background gradients. For experiments based on a stimulated echo pulse sequence, that is preferred for samples with a T_2 short compared to the diffusion time, a diffusion-weighting scheme has been presented that avoids these cross-terms in each of the en- and decoding periods separately. However, this approach suffers from a reduced diffusion-weighting efficiency because the two gradients applied in each of the periods have effectively opposite polarities leading to a partial cancellation. An extension of this scheme is presented that involves an additional gradient pulse in each period and delivers an improved diffusion-weighting efficiency without sacrificing the cross-term compensation. Analytical expressions for the gradient pulse lengths and amplitudes are given for arbitrary timing parameters. MR measurements with artificial (switched) background gradients were performed to test the cross-term compensation capability of the proposed extension. The results show that considerably higher q and b values can be achieved with the extension without changing the timing parameters. The MR measurements yielded identical diffusion coefficients without, with the same, and with different background gradients in the en- and decoding periods demonstrating the cross-term compensation of the presented approach.

Keywords: Background gradients; Cross-term compensation; Diffusion; MAGSTE; PGSTE

1. Introduction

Pulsed-field-gradient NMR [1] has become an important tool for the experimental determination of diffusion (e.g. [2,3]) and has found applications in many fields from material science to medicine (e.g. [4,5]). Many of these applications face the problems associated with background gradients present on a macroscopic or microscopic scale that may be caused by imperfections of the experimental setup, e.g. inhomogeneities of the static magnetic field, or inherent properties of the sample, e.g. susceptibility differences in heterogeneous materials [6]. This applies in particular for the cross-term of the background and the pulsed gradients that varies with the diffusion weighting and therefore may introduce a considerable bias that must be considered in accurate measurements [6].

Because the strength and direction of the background gradients and their spatial distribution is usually unknown, diffusion-weighting sequences have been developed that have a vanishing cross-term at the desired echo time and thereby minimize the disturbing influence of the background gradients (e.g. [2,7]). For instance, Karlicek and Lowe extended a spin-echo preparation by introducing

* Address: Institut für Systemische Neurowissenschaften, Geb. S10, Universitätsklinikum Hamburg-Eppendorf, 20246 Hamburg, Germany. Fax: +49 40 42803 9955.
E-mail address: j.finsterbusch@uke.uni-hamburg.de

1090-7807/$ - see front matter © 2008 Elsevier Inc. All rights reserved.
doi:10.1016/j.jmr.2008.01.002

multiple refocussing pulses and alternating pulsed gradients in-between [8]. Cotts et al. presented a solution for the pulsed-gradient stimulated echo sequence (PGSTE) that is the method of choice for samples with a T_2 relaxation time short compared to the required diffusion time [9]. Their approach involves a refocussing RF pulse in the center of the preparation and readout interval, respectively, each preceded and followed by a diffusion-weighting gradient. However, the cross-term compensation of this technique is only assured if a diffusing spin is exposed to the same background gradient in the preparation and readout intervals, an assumption that often is violated in particular for the long diffusion times accessible with stimulated echoes [10].

Therefore, Sun et al. modified this sequence in order to compensate the cross-terms in each of the intervals separately. This was achieved by using different amplitudes, with a so-called "magic" ratio, for the two gradients around each refocussing RF pulse [11,12]. The cross-term compensation capability of this magic asymmetric gradient stimulated echo (MAGSTE) sequence and the improvements achieved with it for the investigation of heterogeneous samples have been demonstrated recently [13,14]. But because the amplitude ratio required implicates that the two gradients around the refocussing RF have the same polarity, this solution is at a pronounced expense of the diffusion-weighting efficiency.

In the present work, an extension of the standard MAGSTE sequence is presented that replaces one of the two gradients by two successive gradients of opposite polarity which, in sum, have the same duration as the original gradient. It is shown that for an appropriate choice of the relative durations of these two gradients the background-gradient cross-term vanishes as for the standard MAGSTE sequence while the diffusion efficiency is improved, i.e. higher q and b values can be achieved within the same diffusion-weighting time.

2. Theory

In Fig. 1a the basic pulse sequence for the standard MAGSTE sequence is shown. It is based on a stimulated echo that involves a refocussing RF pulse in the middle of each of the preparation and readout intervals and a single gradient pulse before and after each of these RF pulses. To suppress backgrond gradient cross-terms in each of the intervals independently, the gradient pulses must have the same polarity and the "magic" amplitude ratio $|\eta|$ that is given by [11]

$$|\eta| = \frac{\delta^2 + 3\delta\delta_1 + 3\delta_1^2}{5\delta^2 + 9\delta\delta_1 + 3\delta_1^2 + 12(\delta + \delta_1)\delta_2 + 6\delta_2^2} \quad (1)$$

with $|\eta| < 1$. Because the two gradient pulses partially cancel each other, the diffusion-weighting efficiency of this scheme is not optimal.

In the proposed extension (Fig. 1b), the first gradient pulse with the duration δ is replaced by two gradient pulses with opposite polarity, amplitudes of g' and $-g$ and durations of δ' and $\delta - \delta'$, i.e. that effectively cover the same time within the sequence. This could be depicted as a scheme where the first gradient pulse of the standard MAGSTE scheme is compressed in time and an additional gradient pulse is introduced to support the diffusion-weighting effect of the following gradient pulse. Unless explicitely stated, $g' = g$ is assumed and considered in the following sections in detail.

Although not *per se* obvious, the detailed theoretical analysis sketched below shows that for an appropriate choice of δ' the extension (i) has a vanishing background gradient cross-term in each of the preparation and readout interval independently and (ii) delivers higher q values within the given sequence timing.

It should be mentioned that, as outlined previously for the standard MAGSTE sequence [12], the polarity of the gradients in either of the two intervals can be inverted without comprising the background gradient compensation capability of the sequence.

Due to the inherent symmetry of the extended sequence with respect to the middle interval of the stimulated echo, it is sufficient to investigate the preparation interval only without loss of generality. The cross-term with a background gradient in this interval is given by

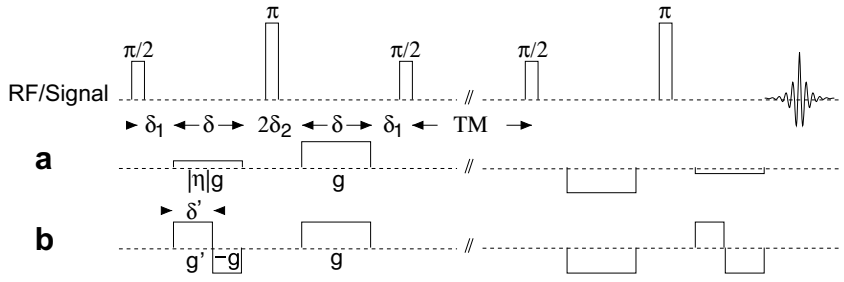

Fig. 1. Basic pulse sequence for (a) the MAGSTE sequence and (b) the proposed extension. Both schemes are based on a stimulated-echo sequence with diffusion-weighting gradients and refocusing RF pulses in the preparation and readout interval prior to and after TM. Whereas MAGSTE involves two gradients with the same duration and polarity in each of the intervals, the extension has three gradients with different duration and polarities. For further details see text.

$$b_{\mathrm{cross}} = \gamma^2 g g_b \left(-\frac{1}{3}\delta'^3 - \delta_1\ \delta'^2 + (2\delta^2 + 4\delta(\delta_1+\delta_2) + \delta_1^2 + 2\delta_2^2 + 4\delta_1\delta_2)\delta' - \delta^3 - 2\delta^2(\delta_1+\delta_2) - \delta(\delta_1+\delta_2)^2 \right) \quad (2)$$

where γ is the gyromagnetic ratio and g_b is the amplitude of the background gradient. For the symmetric case, i.e. $\delta_1 = \delta_2$, Eq. (2) simplifies to

$$b_{\mathrm{cross}} = \gamma^2 g g_b \left(-\frac{1}{3}\delta'^3 - \delta_1\ \delta'^2 + (2\delta^2 + 8\delta\delta_1 + 7\delta_1^2)\delta' - \delta^3 - 4\delta^2\delta_1 - 4\delta\delta_1^2 \right) \quad (3)$$

and further to

$$b_{\mathrm{cross}} = \gamma^2 g g_b \left(-\frac{1}{3}\delta'^3 + 2\delta^2\ \delta' - \delta^3 \right) \quad (4)$$

for $\delta_1 = \delta_2 = 0$.

Solving $b_{\mathrm{cross}} = 0$ in the general case, i.e. $0 \neq \delta_1 \neq \delta_2 \neq 0$ for arbitrary g_b and considering the required boundary condition $0 < \delta' < \delta$ yields the solution

$$\delta' = 2\sqrt{2}(\delta+\delta_1+\delta_2)\cos\left[\frac{1}{3}\arccos\left(-\frac{3\delta^3 + 6\delta^2(2\delta_1+\delta_2) + 3\delta(5\delta_1^2 + 6\delta_1\delta_2 + \delta_2^2) + \delta_1(5\delta_1^2 + 12\delta_1\delta_2 + 6\delta_2^2)}{4\sqrt{2}(\delta+\delta_1+\delta_2)^3}\right) + \frac{\pi}{3}\right] - \delta_1 \quad (5)$$

as derived from Cardano's method for solving cubic polynoms [15,16] and an analysis of the three different solutions obtained (see AppendixA). When assuming $\delta_1 = \delta_2$, δ' simplifies to

$$\delta' = 2\sqrt{2}(\delta+2\delta_1) \times \cos\left[\frac{1}{3}\arccos\left(-\frac{\sqrt{2}(3\delta^3 + 18\delta^2\delta_1 + 36\delta\delta_1^2 + 23\delta_1^3)}{8(\delta+2\delta_1)^3}\right) + \frac{\pi}{3}\right] - \delta_1 \quad (6)$$

and further on to

$$\delta' = 2\sqrt{2}\cos\left(\frac{\pi}{3} + \frac{1}{3}\arccos\left(\frac{3}{8}\sqrt{2}\right)\right)\delta, \quad (7)$$

i.e. $\delta' \approx 0.52\ \delta$, for $\delta_1 = \delta_2 = 0$.

Depending on the type of experiment performed, the gradient integral $q = \int g(t)\,\mathrm{d}t$ or the integral of the squared gradient integral $b = \int (\int g(t')\mathrm{d}t')^2 \mathrm{d}t$ are measures for the diffusion weighting and need to be considered when evaluating the diffusion-weighting efficiency. For the proposed extension, q at the end of the preparation intervall is given by

$$q_{\mathrm{ext}} = 2\ g\ (\delta - \delta'), \quad (8)$$

the b value at the echo time is given by

$$b_{\mathrm{ext}} = 4\gamma^2 g^2 \left(\frac{4}{3}(\delta-\delta')^3 + (2\delta_1 + TM)(\delta-\delta')^2 + \delta_2(\delta-2\delta')^2 + \frac{1}{3}\delta'^3 \right). \quad (9)$$

The corresponding q of the MAGSTE scheme of Sun et al. is given by

$$q_{\mathrm{Sun}} = g\ \delta\ (1 - |\ \eta\ |), \quad (10)$$

yielding a ratio of

$$\frac{q_{\mathrm{ext}}}{q_{\mathrm{Sun}}} = 2\frac{1-\delta'/\delta}{1-|\ \eta\ |}. \quad (11)$$

Solving $q_{\mathrm{ext}}/q_{\mathrm{Sun}} = 1$ for δ_2 delivers only negative solutions. Taking further into account that $q_{\mathrm{ext}}/q_{\mathrm{Sun}} \approx 1.2$ for $\delta_1 = \delta_2 = 0$, it can be concluded that for all positive and finite δ, δ_1, and δ_2 $q_{\mathrm{ext}}/q_{\mathrm{Sun}}$ is greater than 1, i.e. the extension delivers larger q values for any experiment of finite duration.

Concerning the b value, three major contribution can be considered for both schemes: the b values accumulated during (i) the preparation interval (b_{prep}), (ii) the readout intervals (b_{readout}), and (iii) the middle interval TM (b_{TM}). Due to the symmetry of the sequence, $b_{\mathrm{prep}} = b_{\mathrm{readout}}$ for both schemes. Because there is no effective diffusion weighting during TM, b_{TM} is given by $q_{\max}^2 \cdot TM$ where $q_{\max}$ is the gradient integral accumulated during the preparation interval and is given by Eq. (8) and (10), respectively. Because $q_{\mathrm{ext}}/q_{\mathrm{Sun}}$ has been shown to be greater than 1, b_{TM} is always larger for the propsed extension.

An analogue, analytical comparison of b_{prep} is difficult due to the cos-arccos in Eq. (5) and the b value of the standard MAGSTE scheme that depends on δ, δ_1, and δ_2 in powers of 4. Therefore, b_{prep} was compared on the basis of numerical calculations.

Some results for the general case $g' \neq g$ that may be relevant in practice, e.g. when considering discrete gradient raster times, are summarized in Appendix B.

3. Experimental

Parts of the analytical calculations and numerical simulations were performed with Maple (version 9.5.2, Waterloo Maple Inc., Waterloo, Ontario, Canada).

Self-written algorithms in IDL (version 5.5a, Research Systems Inc., Boulder, CO, USA) were used (i) to demonstrate the temporal evolution of the b value as well as the gradient crossterm of a background gradient and the diffusion-weighting gradient pulses for both diffusion-weighting schemes and (ii) to calculate the b value of the preparation

interval, b_{prep}, of both schemes. In the latter case, δ, δ_1, and δ_2 were varied independently with δ running from 0.2 to 1000.0 ms in steps of 0.2 ms and δ_1 as well as δ_2 from 0.0 to 100.0 ms in steps of 0.1 ms, respectively.

MR experiments were performed on a 3T whole-body MR system (Magnetom Trio, Siemens Medical Solutions) on doped water phantoms and a kohlrabi (stem cabbage). 2D Fourier transform imaging versions of the sequences shown in Fig. 1a and b were used involving slice-selective RF pulses, phase- and frequency-encoding gradient pulses applied after the diffusion weighting, and repetition of the full sequence with different amplitudes of the phase-encoding gradient pulse. To suppress unwanted coherence pathways, spoiler gradient pulses were applied around the refocussing RF excitations with different amplitudes in the preparation and readout interval.

To simulate background gradients in the experiment, pulsed field gradients in the slice-selection direction were switched with the same ($+1$ mT m^{-1}) or different amplitudes (-1 mT m^{-1} and $+2$ mT m^{-1}) during the preparation and readout interval, respectively.

Unless otherwise noted, parameters for the imaging experiments were an in-plane resolution of 2×2 mm^2 and 5×5 mm^2 for the water phantoms and the kohlrabi, respectively, a slice thickness of 5 mm, an echo time (TE) of 150 ms, a mixing time (TM) of 100 ms, and a repetition time (TR) of 2000 ms. Diffusion weighting was performed in slice direction with b values of 500, 1000, 1500, and 2000 s mm^{-2}, an δ of 20 ms, and an $|\eta|$ of 0.22 and a δ' of 11.0 ms, respectively, for the used timing. The apparent diffusion coefficient (ADC) was calculated during the image reconstruction on a voxel-by-voxel basis using software provided by the manufacturer. The mean ADC value in a region-of-interest in the center of the phantom was used for the evaluation.

4. Results

Results of the numerical simulations shown in Fig. 2 demonstrate the temporal evolution of the relevant terms for both schemes in the preparation interval. The cross-term vanishes at the end of the interval for both cases (Fig. 2b) with the extension showing higher intermediate values caused by the higher gradient amplitudes applied in the first half of the interval. Because the gradient integral of the background gradient also vanishes at this time due to the refocusing RF in the middle of the interval, additional contributions to the cross-term that could arise during TM, are avoided [9]. For the parameters used, the b value of the diffusion-weighting gradient, however, exhibits a markedly higher value at the end of the interval for the extension (Fig. 2c) reflecting an improved efficiency. It should be emphasized that in addition to the higher value, the slope of the b curve is also steeper compared to the standard MAGSTE scheme of Sun et al. Thus, the b value that accumulates during the TM interval, that is proportional to this slope, is also increased which further improves the diffusion-weighting efficiency. The temporal

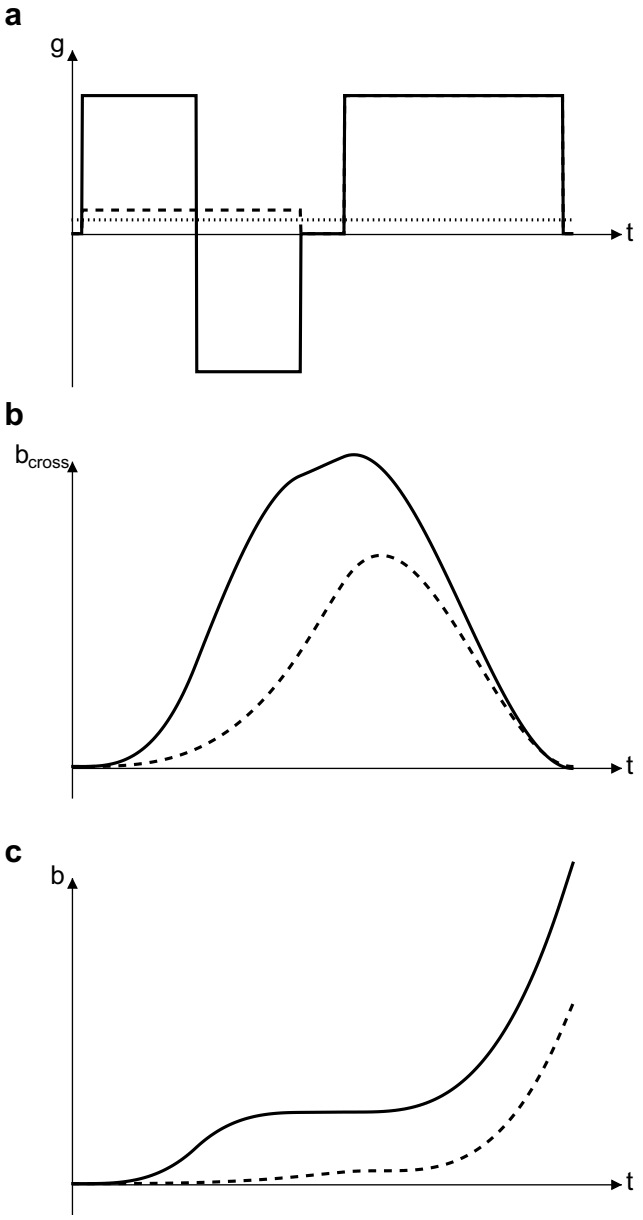

Fig. 2. Schematic time courses for MAGSTE (dashed) and the proposed extension (solid): (a) the diffusion-weighting gradients and an assumed background gradient (dotted), (b) the cross-term of the diffusion and background gradients shown in (a), and (c) the b value of the diffusion gradients. The calculations were performed with a δ of 20.0 ms, a δ_1 of 1.0 ms, and a δ_2 of 2.0 ms yielding $|\eta| \approx 0.17$ and $\delta' \approx 10.5$ ms. For these parameters the b value and its slope at the end of the shown interval are larger by factors of about 1.8 and 1.3, respectively, for the extension. The relative amplitude of the background gradient was 10%.

evolution during the readout interval is obtained by mirroring gradient and cross-term plots (Fig. 2a and b) along the time axis and the b value plot along both, the time axis and vertically, respectively. This means that as for the preparation interval an identical b value gain is also achieved in the readout interval for the extension.

The ratio δ'/δ, with δ' given by Eq. (5), is plotted in Fig. 3a for the general case ($0 \neq \delta_1 \neq \delta_2 \neq 0$) for two values of δ. For shorter δ, the ratio is rather independent of δ_1 and

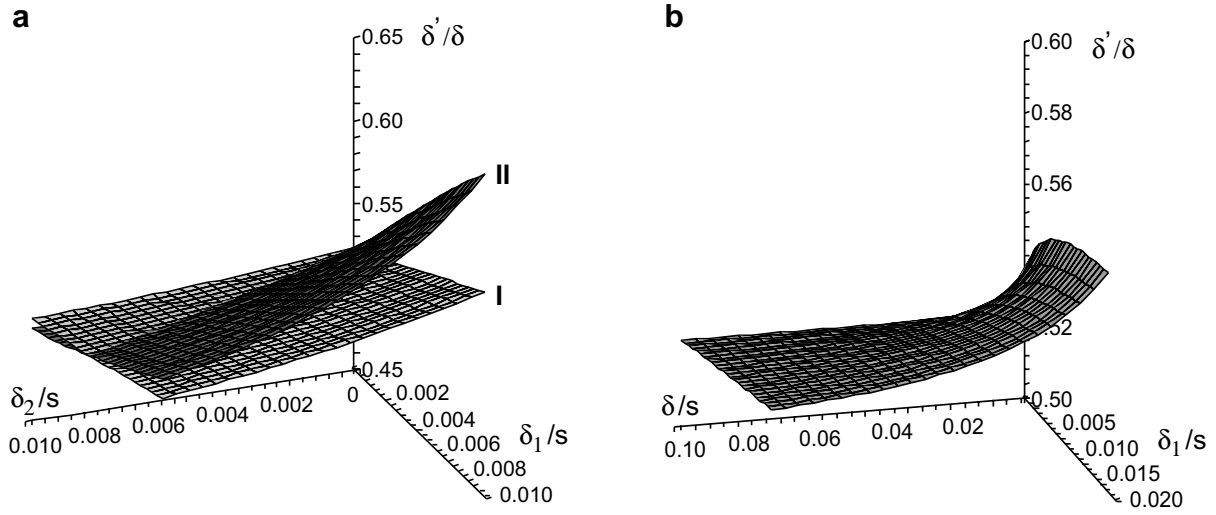

Fig. 3. δ'/δ for which the background-gradient cross-term compensation is achieved for the extension as a function of (a) δ_1 and δ_2 for a δ of 10 ms (light grey, I) and 25 ms (dark grey, II) and (b) δ and δ_1 with $\delta_2 = \delta_1$.

δ_2 while for longer δ the ratio increases for a combination of short δ_2 and longer δ_1. In the symmetric case ($\delta_1 = \delta_2 \neq 0$) shown in Fig. 3b, the ratio increases for shorter δ with a local maximum for intermediate δ_1. Values of δ'/δ for typical experimental setups can be estimated to be in the range between 0.5 and 0.6.

For the symmetric case, that is expected to be more common in practice, results concerning the diffusion-weighting efficiency are shown in Fig. 4 presenting ratios of corresponding values for the extension and the standard MAGSTE scheme. For q^2 (Fig. 4a), typical values are around 1.2 up to 1.4 with large values for short $\delta_1 = \delta_2$ over a wide range of δ and smaller values for the more unrealistic combination of short δ with long $\delta_1 = \delta_2$. q^2 is important with respect to the fact that it represents the slope of the temporal b value evolution in the middle interval TM where usually a significant amount of the required b value is accumulated. Thus, q^2 is a measure for the diffusion weighting efficiency in the limit of infinite TM with a gain of about 20% up to 40% compared to the standard MAGSTE scheme. The ratio of the b values obtained with the two schemes for finite TM are shown in Fig. 4b. Most of the values are comparable or slightly below the q^2 but in particular for shorter TM even higher values of up to a gain of 50% for the extension are obtained. This is due to the higher b value that is already accumulated in the preparation interval, i.e. before the middle interval, as for instance can be seen in Fig. 2c.

The numerical calculations of b_{prep} performed over a larger parameter range than that shown in Fig. 4 and for the general case with $\delta_1 \neq \delta_2$ revealed a superior diffusion-weighting efficiency of the extension for all parameter combinations investigated with a maximum gain of about 105%, i.e. a more than doubled b_{prep}, for a δ of 4.0 ms and $\delta_1 = \delta_2 = 0$ ms. For some, extreme parameter combinations b_{prep} of the extension was very close to that of stan-

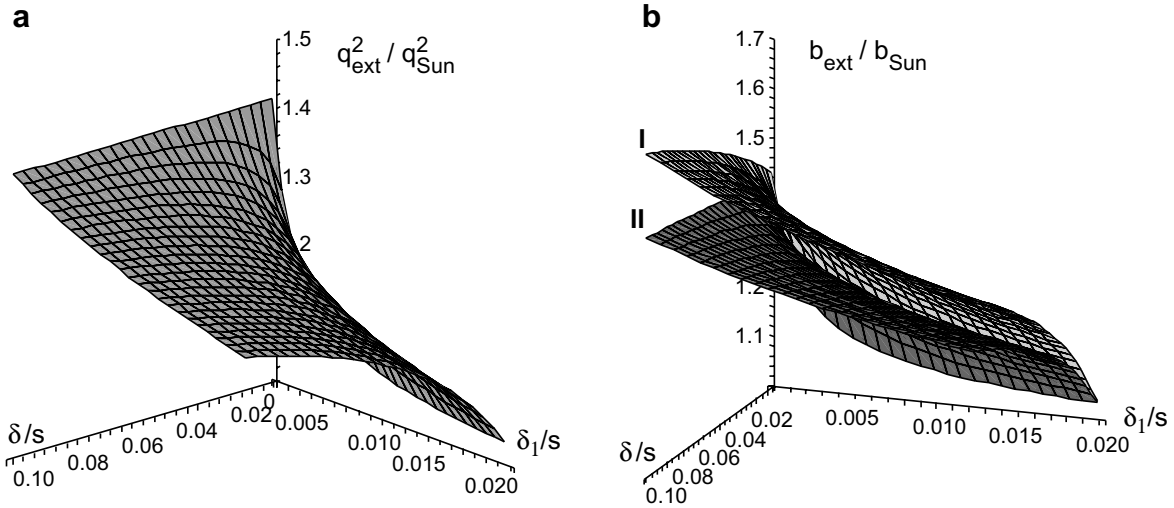

Fig. 4. Relative (a) q^2 and (b) b values of the extension compared to the MAGSTE scheme of Sun et al. for a TM of 100 ms (light grey, I) and 500 ms (dark grey, II) as a function of δ and δ_1 with $\delta_2 = \delta_1$ and background gradient cross-term compensation.

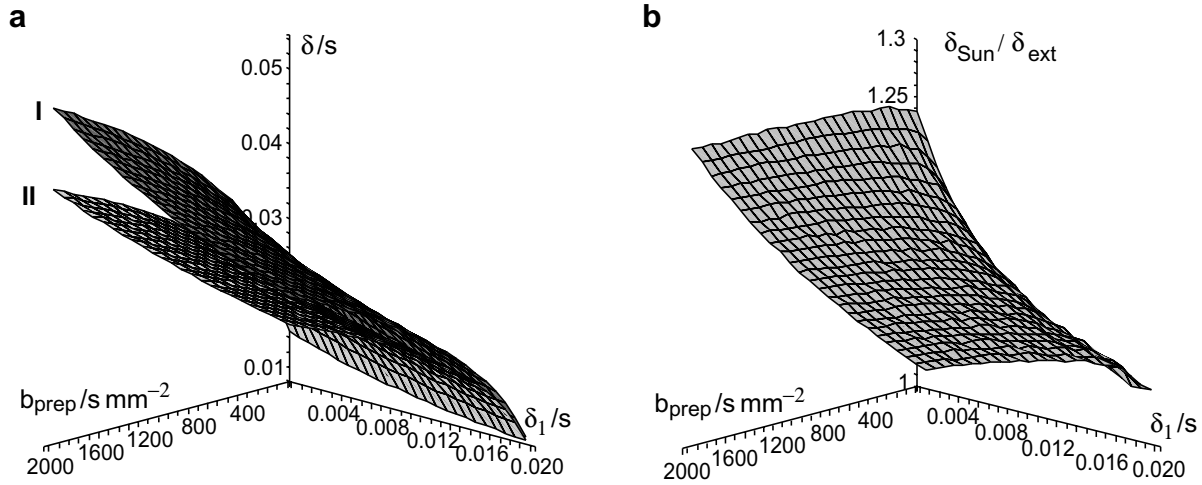

Fig. 5. (a) Gradient durations δ required to achieve a given b_{prep} for standard MAGSTE (dark gray, I) and the extension (light gray, II) and (b) their ratio. The symmetric case ($\delta_1 = \delta_2$) and a gradient amplitude g of 30 mT m^{-1} were assumed.

dard MAGSTE, e.g for $\delta = 0.4$ ms and $\delta_1 = \delta_2 = 100.0$ ms the gain was below 1%. However, this combination can be considered to be rather unusual for real experiments.

In Fig. 5, gradient durations δ are compared for the standard MAGSTE sequence and the extension depending on a given b_{prep}. A several ms or about 10–20% longer δ is required for standard MAGSTE to achieve the same b_{prep} for a maximum amplitude of the diffusion gradients of 30 mT m^{-1}, i.e. typical gradient systems available on whole-body MR systems. For stronger gradient systems, similar results can be found with the δ ratio slightly decreasing with the maximum gradient amplitude. For instance, the δ for the standard MAGSTE sequence is still up to 22% and 18% longer compared to the extension for gradient amplitudes of 200 and 500 mT m^{-1}, respectively (data not shown).

Fig. 6 presents the maps of the diffusion coefficent obtained in the experiments on a water phantom for standard MAGSTE and the extension. As expected, the measured mean diffusion coefficent (2.081×10^{-3} mm^2 s^{-1}) does not significantly change in the presence of constant or variable background gradients for standard MAGSTE compared to the measurement performed without background gradient (±0.8%, Fig. 6a–c). This is also observed for the extension (2.094×10^{-3} mm^2 s^{-1}, ±0.6%, Fig. 6d–f) demonstrating its background gradient cross-term compensation capability. The minor difference in the mean diffusion coefficient of 0.4% between the two schemes could be caused by a slightly different gradient scaling along the covered gradient amplitude range and/or for positive and negative gradient polarity that are expected to affect the two schemes in a different manner. Different value-to-noise

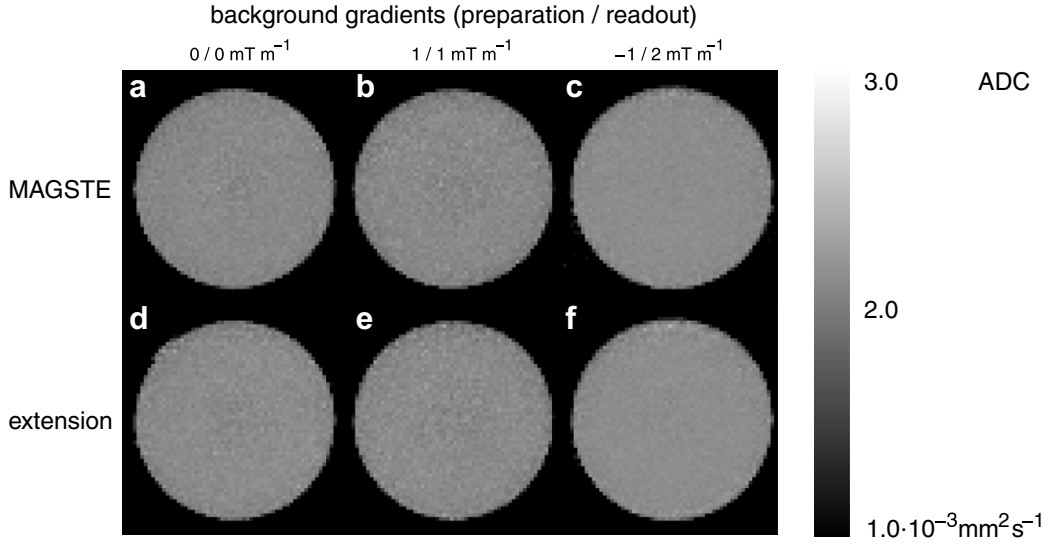

Fig. 6. Maps of the diffusion coefficient measured on a water phantom with (a–c) the MAGSTE sequence and (d–f) the presented extension. Artificial background gradients were applied with (b, e) an amplitude of +1 mT/m in both, preparation and readout, intervals and (c, f) amplitudes of −1 mT/m and +2 mT/m in the preparation and readout interval, respectively. Diffusion-weighting was performed in slice direction. Gray scaling of all maps is identical and according to the gray scale bar on the right.

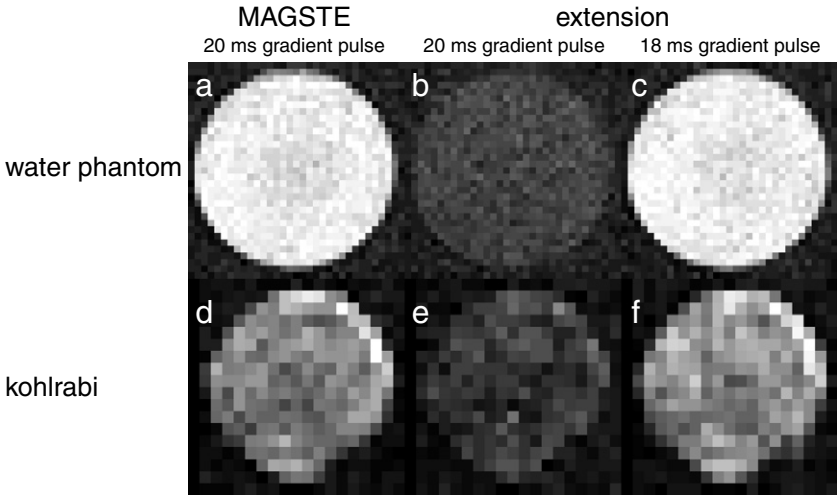

Fig. 7. Diffusion-weighted MR images of (a–c) a water phanom and (d–f) a kohlrabi acquired with (a, d) standard MAGSTE with a b value of 2000 s mm^{-2}, (b, e) the proposed extension with a b value of 2600 s mm^{-2} obtained for the same gradient duration δ and amplitude g as used for (a), and (c, f) the proposed extension with a b value of 2000 s mm^{-2} obtained with a gradient duration δ reduced from 20 to 18 ms and a correspondingly 8 ms shorter echo time compared to (a). Images of the same phantom have identical gray scalings. The signal-to-noise ratio in (b) and (e) is reduced by about 60% and 50% compared to (a) and (d), respectively, due to the stronger diffusion weighting. While the signal intensity in (f) is increased by about 10% compared to (d) because of the shorter echo time, a significant improvement is not observed for the water phantom with its much longer T_2 relaxation time.

ratios were observed in the maps shown in Fig. 6 due to the interaction of the background gradients with the slice-selection gradient pulses that increased or reduced the effective gradients during the RF excitations resulting in narrowed or broadened slice thicknesses.

The measurements underlying Fig. 6 were performed with different gradient amplitudes for the standard MAGSTE and the extension due to the improved diffusion-weighting efficiency of the latter technique. The higher b value or shorter δ achievable with the extension when using the same gradient amplitude g is demonstrated in Fig. 7 for a water and kohlrabi phantom. For the given g, a b value of 2600 s mm^{-2} can be realized in the example shown (Fig. 7b and e) compared to the 2000 s mm^{-2} obtained for standard MAGSTE (Fig. 7a and d) for an identical timing. On the other hand, when targeting a given b value, a shorter δ can be used with the extension (Fig. 7c and f) that allows to decrease the echo time and thereby reduces T_2 relaxation losses, in particular in samples with shorter T_2 (Fig. 7f).

5. Discussion

The standard MAGSTE scheme of Sun et al. has been extended by a third gradient pulse in the preparation and readout interval that also ensures compensation of background gradient cross-terms for an appropriate gradient timing. The extension offers higher q values and, although no analytical derivation could be presented for a general prove, the results obtained in numerical simulations strongly indicate that it is very likely to obtain a gain in the b efficiency as well for the timing parameters present in PGSTE experiments. Due to the improved efficiency, the extension can facilitate the access to high b values, in particular on whole-body MR systems where the maximum gradient amplitude available is relatively low. Alternatively, the extension can be used with shorter echo times in order to minimize relaxation-related signal loss which is particularly important because the underlying stimulated echo sequence usually is applied in samples with short T_2.

It should be emphasized that both, the MAGSTE sequence and its extension, only compensate background gradients that vary between the preparation and the readout interval but are constant during each of the preparation and the readout intervals. This may hamper their applicability on whole-body MR systems that usually require rather long gradient pulses to achieve sufficient diffusion weighting. However, due to its better diffusion-weighting efficiency, the proposed extension may help to shorten gradient pulses and interval durations and to reduce corresponding artifacts.

Whereas the theoretical derivations and results presented deal with rectangular gradient shapes, the consideration of finite ramp times, i.e trapezoidal gradients, as has been investigated for standard MAGSTE [12], is straightforward. It can be performed following the derivation and argumentation sketched in this work, however, the calculations soon become quite tedious and the length of the terms for δ' and b increases considerably. Solutions for other gradient shapes, like sinusoidal [12], are also expected to be found but are beyond the scope of this manuscript as well.

A potentially more interesting modification could take the specific needs for imaging sequences into account. They employ additional gradients for spatial encoding that, e.g. for phase encoding, must be applied prior to the echo maximum and thereby reduce the time available for the last diffusion-weighting gradient pulse of the MAGSTE sequence. This shortening is even more pronounced for imaging sequences that cover several gradient echoes per shot, like echo-planar imaging [17]. This could be solved with the

results presented for standard MAGSTE or the extension so far by including the time required for the corresponding gradients into δ_1 but yields an unneeded delay at the beginning of the readout interval where δ_1 also appears with the corresponding relaxation losses. Thus, the assumption of an asymmetric timing seems to be the better approach but considering the lengthy results obtained already in this work, it may be difficult to achieve an useful analytical solution for this case.

6. Conclusions

The MAGSTE method of Sun et al. proposed to compensate background-gradient cross-terms in stimulated-echo-based diffusion-weighted MR, has been extended by additional gradient pulses. It has been demonstrated that the extension offers an increased diffusion-weighting efficiency without sacrificing the cross-term compensation capability. Thus, it may help to further improve the accuracy of diffusion coefficient measurements in heterogeneous samples where the required diffusion time is long compared to the transverse relaxation time.

Acknowledgments

Parts of this work were supported by Deutsche Forschungsgemeinschaft and Bundesministerium für Bildung und Forschung (Neuroimage Nord).

Appendix A

The derivation of Eq. (5) and the analysis showing that it obeys the required boundary condition $0 < \delta' < \delta$ is sketched in the following paragraphs.

The cross-term of Eq. (2) is a cubic polynom of δ'. Using the method of Cardano [15,16], the solutions of the equation

$$c_3x^3 + c_2x^2 + c_1x + c_0 = 0 \tag{A.1}$$

are real and given by

$$\begin{aligned}
x_1 &= -\sqrt{-\frac{4}{3}p}\cos\left(\frac{1}{3}\arccos\left(-\frac{q}{2}\sqrt{-\frac{27}{p^3}}\right)+\frac{\pi}{3}\right)-\frac{c_2}{3c_3}\\
x_2 &= \sqrt{-\frac{4}{3}p}\cos\left(\frac{1}{3}\arccos\left(-\frac{q}{2}\sqrt{-\frac{27}{p^3}}\right)\right)-\frac{c_2}{3c_3}\\
x_3 &= -\sqrt{-\frac{4}{3}p}\cos\left(\frac{1}{3}\arccos\left(-\frac{q}{2}\sqrt{-\frac{27}{p^3}}\right)-\frac{\pi}{3}\right)-\frac{c_2}{3c_3}
\end{aligned} \tag{A.2}$$

with

$$\begin{aligned}
p &= \frac{3c_3c_1 - c_2^2}{3c_3^2}\\
q &= \frac{2c_2^3}{27c_3^3} - \frac{c_2c_1}{3c_3^2} + \frac{c_0}{c_3}
\end{aligned} \tag{A.3}$$

if, as in case of the zero-crossings of Eq. (2),

$$4p^3 + 27q^2 < 0. \tag{A.4}$$

Considering the zero-crossings of Eq. (2), it is straightforward to show that Eq. (A.4) is fulfilled for positive δ, δ_1, and δ_2, i.e. that the solutions of δ' are given by Eq. (A.2).

Whether one (or more) of the x_i defined in Eq. (A.2) obeys the boundary condition $0 < x_i < \delta$ is not obvious and requires to consider the individual contributions to the x_i. The argument of the arccos in Eq. (A.2) is the same for all solutions and is given by

$$-\frac{q}{2}\sqrt{-\frac{27}{p^3}} = -\frac{\sqrt{2}(3\delta^3 + 6\delta^2(2\delta_1+\delta_2) + 3\delta(5\delta_1^2 + 6\delta_1\delta_2 + \delta_2^2) + \delta_1(5\delta_1^2 + 12\delta_1\delta_2 + 6\delta_2^2)}{8(\delta+\delta_1+\delta_2)^3}, \tag{A.5}$$

i.e. is negative for all positive δ, δ_1, and δ_2. Thus, the arccos value can be chosen within the interval $[\pi/2, \pi]$. Considering the factor 1/3 and the additional term $\pm\pi/3$ for x_1 and x_3, respectively, the argument of the cos must be within the intervals $[\pi/2, 2\pi/3]$ for x_1, $[\pi/6, \pi/3]$ for x_2, and $[-\pi/6, 0]$ for x_3, respectively, yielding negative cos values for x_1 and positive cos values for x_2 and x_3. Together with the factor

$$\pm\sqrt{-\frac{4}{3}p} = \pm 2\sqrt{2}(\delta+\delta_1+\delta_2) \tag{A.6}$$

it can be seen that x_3 is negative for all positive δ, δ_1, and δ_2 and therefore is not a suitable solution. Because

$$\begin{aligned}
\lim_{\delta_2\to\infty} x_1 &= \frac{\delta}{2}\\
\lim_{\delta_2\to\infty} x_2 &= \infty,
\end{aligned} \tag{A.7}$$

x_1 is the only solution that may in general be within the desired boundaries.

To show that the requested boundary conditions are fulfilled for x_1, $x_1 = \delta$ is solved for δ_2 yielding

$$(\delta_2)_{1,2} = -(\delta+\delta_1) \pm \frac{1}{3}\sqrt{3}\sqrt{\delta^2 + 3\delta\delta_1 + 3\delta_1^2}. \tag{A.8}$$

Both values are negative for positive δ and δ_1, i.e. with the limit of Eq. (A.7), it is shown that x_1 does not exceed δ for positive δ_2. Because $x_1 = \delta/2$ has also no solutions for positive δ_2, it can be concluded that x_1 is within $[\delta/2, \delta[$ for all positive δ, δ_1, and δ_2.

Appendix B

In case the δ' according to Eq. (5) cannot be used in the desired experiment, e.g. because it is not a multiple of the MR system's gradient raster time or due to other hardware or experimental considerations, the proposed extension can be used in the more general case with $g' \neq g$. The corresponding results are summarized here without showing the straightforward derivation.

Given δ', the gradient amplitude of the first and last gradient shown in Fig. 1b must be chosen as

$$g' = g\frac{6\delta^2(2\delta_{1+2} - \delta' + \delta) + 6\delta\delta_{1+2}(\delta_{1+2} - 2\delta') - 3\delta'(\delta_1^2 - 4\delta_1\delta_2 - 2\delta_2^2) + \delta'^2(3\delta_1 + \delta')}{\delta'\left(6(\delta + \delta_{1+2})^2 - \delta'^2 - 3\delta_1\delta' - 3\delta_1^2\right)} \tag{A.9}$$

with $\delta_{1+2} = \delta_1 + \delta_2$ to ensure cross-term compensation. If δ' is larger than the value given by Eq. (5), g' is lower than g. For a gradient raster time of 10 μs, rounding up the δ' given by Eq. (5) delivers typically $g'/g > 0.99$ with a marginal influence on the diffusion-weighting efficiency.

The b value for the general case is given by

$$\begin{aligned} b'_{\text{ext}} = \gamma^2 g^2 \ & \left(4\delta^2\left(2(\delta_1 + \delta_2 - \delta') + TM + \frac{4}{3}\delta\right) - 4\delta\delta'(2\delta_1 + 2\delta_2 - \delta' + TM) + \delta'^2\left(8\delta_1 + 4\delta_2 + TM - \frac{2}{3}\delta'\right)\right) \\ & + \gamma^2 g\ g'\ \delta'(2\delta'(4\delta + 2\delta_1 + 4\delta_2 + TM - \delta') - 4\delta(2\delta + 2\delta_1 + 2\delta_2 + TM)) \\ & + \gamma^2 g'^2\ \delta'^2\left(4\delta + 2\delta_1 + 4\delta_2 + TM - \frac{4}{3}\delta'\right). \end{aligned} \tag{A.10}$$

References

[1] E.O. Stejskal, J.E. Tanner, Spin diffusion measurements: spin echoes in the presence of a time-dependent field gradient, J. Chem. Phys. 42 (1965) 288–292.

[2] W.S. Price, Pulsed field gradient nuclear magnetic resonance as a tool for studying translational diffusion: Part I. Basic theory, Concepts Magn. Reson. 9 (1997) 299–336.

[3] W.S. Price, Pulsed field gradient nuclear magnetic resonance as a tool for studying translational diffusion: Part II. Experimental aspects, Concepts Magn. Reson. A 10 (1998) 197–237.

[4] J. Kärger, P. Heitjans (Eds.), Diffusion in Condensed Matter – Methods, Materials, Models, Springer-Verlag, Berlin–Heidelberg, 2005.

[5] T. Moritani, S. Ekholm, P.-L. Westesson, Diffusion-Weighted MR Imaging of the Brain, Springer-Verlag, Berlin–Heidelberg, 2005.

[6] J. Zhong, R.P. Kennan, J.C. Gore, Effects of susceptibility variations on NMR measurements of diffusion, J. Magn. Reson. 95 (1991) 133–139.

[7] G. Zheng, W.S. Price, Suppression of background gradients in (B0 gradient-based) NMR diffusion experiments, Concepts Magn. Reson. A 30 (2007) 261–277.

[8] R.F. Karlicek, I.J. Lowe, A modified pulsed gradient technique for measuring diffusion in the presence of large background gradients, J. Magn. Reson. 37 (1980) 75–91.

[9] R.M. Cotts, M.J.R. Hoch, T. Sun, J.T. Markert, Pulsed field gradient stimulated echo methods for improved NMR diffusion measurements in heterogeneous systems, J. Magn. Reson. 83 (1989) 252–266.

[10] J.G. Seland, G.H. Sørland, K. Zick, B. Hafskjold, Diffusion measurements at long observation times in the presence of spatially variable internal magnetic field gradients, J. Magn. Reson. 146 (2000) 14–19.

[11] P.Z. Sun, J.G. Seland, D. Cory, Background gradient suppression in pulsed gradient stimulated echo measurements, J. Magn. Reson. 161 (2003) 168–173.

[12] P.Z. Sun, A.S. Seth, J. Zhou, Analysis of the magic asymmetric gradient stimulated echo sequence with shaped gradients, J. Magn. Reson. 171 (2004) 324–329.

[13] P. Galvosas, F. Stallmach, J. Kärger, Background gradient suppression in stimulated echo NMR diffusion studies using magic pulsed field gradient ratios, J. Magn. Reson. 166 (2004) 164–173.

[14] P.Z. Sun, Improved diffusion measurement in heterogeneous systems using the magic asymmetric gradient stimulated echo (MAGSTE) technique, J. Magn. Reson. 187 (2007) 177–183.

[15] W.S. Anglin, J. Lambek, The heritage of Thales, chapter 24 (Mathematics in the Renaissance), Springer-Verlag, New York, 1995.

[16] I.N. Bronstein, K.A. Semendjajew, Taschenbuch der Mathematik, Nauka, Moscow and BSB B.G. Teubner Verlagsgesellschaft, Leipzig, 1985.

[17] P. Mansfield, Multi-planar image formation using NMR spin echoes, J. Phys. C 10 (1977) 349–352.